THE ASTROPHYSICAL JOURNAL, 391:L99–L103, 1992 June 1

CHEMISTRY IN CIRCUMSTELLAR DISKS: CS TOWARD HL TAURI

GEOFFREY A. BLAKE,[1] EWINE F. VAN DISHOECK,[1,2] AND ANNEILA I. SARGENT[3]
Received 1991 December 27; accepted 1992 March 19

ABSTRACT

High-resolution millimeter-wave aperture synthesis images of the CS $J = 2 \rightarrow 1$ and dust continuum emission toward the young star HL Tauri have been combined with single-dish spectra of the higher J CS transitions in order to probe the chemical and physical structure of circumstellar material in this source. We find that the extended molecular cloud surrounding HL Tau is similar to other Taurus dark cloud cores, having $T_{\rm kinetic} \approx$ 10–20 K, $n_{\rm H_2} \approx 10^4$–10^5 cm^{-3}, and $x({\rm CS}) = N({\rm CS})/N({\rm H_2}) \approx (1\text{–}2) \times 10^{-8}$. In contrast, the gas-phase CS abundance in the circumstellar disk is depleted by factors of at least 25–50, and perhaps considerably more. These results are consistent with substantial depletion onto grains, or a transition from kinetically controlled chemistry in the molecular cloud to thermodynamically controlled chemistry in the outer regions of the circumstellar disk.

Dust continuum emission at 3.06 mm, although unresolved in a 3″.0 beam, appears centered on the stellar position; combined with other millimeter-wave measurements its intensity indicates an emissivity index of $\beta = 1.2 \pm 0.3$. This β may reflect grain growth via depletion and aggregation or compositional evolution, and suggests that the 3.06 mm dust opacity exceeds unity within 8–10 AU of HL Tauri. Even at millimeter and submillimeter wavelengths, observational studies of other high dipole moment molecules in circumstellar disks may also be hampered by the combination of grain mantle depletion and dust opacity structure in sources viewed nearly edge-on.

Subject headings: circumstellar matter — ISM: molecules — stars: pre–main-sequence

1. INTRODUCTION

Observations of molecular clouds in the Galaxy have revealed that a large fraction of young low-mass stars are associated with circumstellar material which probably resides in disklike structures (Shu, Adams, & Lizano 1987). Infrared, far-infrared, and millimeter single-dish continuum data combined with interferometric images of both the continuum and CO emission (Sargent & Beckwith 1987; Weintraub, Masson, & Zuckerman 1989; Strom et al. 1989; Beckwith et al. 1990; Strom, Edwards, & Strutskie 1992) show that the properties of these putative disks are similar to those assumed for the presolar nebula, and they therefore provide stringent tests of theories of stellar and planetary genesis. It is usually assumed that the gas and dust have the same physical structure since at the densities inferred for disks they should be thermally coupled. This conjecture has not been tested in detail, however.

Little is known about the chemical structure of circumstellar disks on small size scales. Chemical gradients might be expected if molecules are selectively depleted onto grain mantles in the colder regions or if there is a change from kinetically controlled "interstellar" chemistry in the outer part to equilbrium-dominated "nebular" chemistry in the inner part (see, e.g., van Dishoeck et al. 1992a). Better constraints on the chemical and physical structure of the dense gas and dust surrounding young stars require measurements of molecules with larger dipole moments. As a first step in that direction, we present here interferometric observations of the $J = 2 \rightarrow 1$ emission line of the CS molecule in HL Tauri, one of the nearest and best-studied circumstellar disks. Based on the measured CO and ^{13}CO line fluxes (Beckwith et al. 1986; Sargent & Beckwith 1991) and the CS/CO ratio in interstellar clouds, CS was expected to be readily detectable. It has in fact been observed in a CS $2 \rightarrow 1$ interferometric survey of 11 protostellar *IRAS* sources by Ohashi et al. (1991). We have combined interferometric CS $2 \rightarrow 1$ data with single-dish observations of the CS $2 \rightarrow 1$, $3 \rightarrow 2$, $5 \rightarrow 4$, and $7 \rightarrow 6$ lines in 12″–25″ beams to derive the temperatures and densities sampled by the CS emission. The CS/CO ratio in circumstellar gas is also of interest for comparison with cometary comae, where both molecules have been observed.

Our aperture synthesis observations simultaneously map the continuum flux at 3.06 mm. Together with published 2.72 and 1.37 mm fluxes, this provides a measure of dust opacity variation at longer millimeter wavelengths (cf. Ohashi et al. 1991). The opacity function in turn reflects the nature of grain growth and composition in circumstellar disks.

2. OBSERVATIONS

The CS $J = 2 \rightarrow 1$ line and the $\lambda = 3.06$ mm continuum were observed toward HL Tau between 1989 November and 1991 March with the Owens Valley Radio Observatory (OVRO) millimeter wave interferometer. Seven configurations of the three 10.4 m telescopes, with unprojected baselines up to 200 m E-W and 140 m N-S, produced a synthesized beam of 3″.15 × 2″.80 at P.A. −16°. At 3.06 mm the primary beam size is 74″. SIS receivers cooled to 4 K gave system temperatures of 100–400 K (SSB). Two 32 × 50 kHz and 32 × 1 MHz filter banks, centered on 6.6 km s^{-1}, provided velocity resolutions of 0.15 and 3.1 km s^{-1}, respectively. Simultaneous continuum measurements were made using a wide-band (375 MHz) correlator.

Spectral line and continuum maps were generated by the NRAO AIPS software package. The continuum source 3C 120

[1] Division of Geological and Planetary Sciences, California Institute of Technology 170-25, Pasadena, CA 91125.
[2] Leiden Observatory, P.O. Box 9513, 2300 RA Leiden, The Netherlands.
[3] Division of Physics, Mathematics and Astronomy, California Institute of Technology 105-24, Pasadena, CA 91125.

served as the instrumental phase calibrator, whereas amplitude calibrations were based upon regular observations of 3C 273, 3C 84, and Uranus. The overall uncertainties in fluxes and positions are estimated to be 15% and 1″.

Supporting single-dish observations were obtained in 1989 December and 1990 November at the Caltech Submillimeter Observatory (CSO), and in 1991 May at the IRAM 30 m telescope. At the CSO we searched for the CS 5–4 and 7–6 lines using the facility SIS receivers. The CSO beam sizes at these frequencies were 28″ and 20″, and the main-beam efficiencies were 0.72 and 0.60. At the IRAM 30 m telescope, the CS 2–1, 3–2, and 5–4 lines were observed simultaneously, thereby minimizing any pointing differences. Beam sizes were 25″, 17″, and 12″, with main-beam efficiencies of 0.61, 0.57, and 0.46.

3. RESULTS

3.1. *Continuum Emission*

In Figure 1 (Plate L8) OVRO interferometer contour maps of the 3.06 mm dust continuum and integrated CS emission from HL Tau are presented against gray-scale images of the ^{13}CO $J = 1 \rightarrow 0$ emission over the same velocity ranges. Continuum emission from HL Tau at 3″ resolution and $\lambda = 3.06$ mm, like that at 2.72 mm in a 2.″7 beam (Sargent & Beckwith 1991), is unresolved and centered on the star. The integrated flux at 3.06 mm is 75 ± 10 mJy, significantly lower than at 2.72 mm, 112 ± 15 mJy. The convolved source size is only 383×445 AU for an assumed distance of 140 pc (Elias 1978). Gaussian fits give a formal upper limit to the deconcolved source size of 150–200 AU.

3.2. *CS $J = 2 \rightarrow 1$ Interferometer Maps*

To achieve maximum sensitivity, the CS maps were produced with natural weighting of the (u, v) data, yielding a $4.''9 \times 4.''2$ beam at P.A. $-76.°7$. At millimeter wavelengths the CS and continuum emission from HL Tau are comparable in $\sim$1–10 km s^{-1} bandwidths. Subtraction of a model continuum source therefore has a significant impact on the CS images. In unprocessed maps the emission is nearly centered on the stellar position except in narrow velocity ranges (Fig. 1); when the continuum flux is subtracted, the CS emission peak is always displaced roughly 3″ to the west of HL Tau (Ohashi et al. 1991).

At first glance, the overall morphology and orientation of the CS emission is similar to that of ^{13}CO (Sargent & Beckwith 1991). Both molecules exhibit a central condensation near the stellar position, flanked by additional concentrations to the NW and S. No continuum emission is detected from the NW and S sources, implying very low masses. The central structure is marginally resolved, with a nominal source size of $2.''8 \times 5.''0$ (390×700 AU) at P.A. 165°. The brightest CS emission occurs at $V_{LSR} \approx 8.1$ km s^{-1}, similar to the ^{12}CO images of HL Tau (Beckwith et al. 1986), but somewhat larger than the ^{13}CO central velocity of 6.6 km s^{-1}. The peak positions of the ^{13}CO and CS emission are also different in the narrower velocity range images (Figs. 1*b*, 1*c*).

Because of the unexpected peak velocity, the CS line is not centered in the 32×50 kHz back end, and a full analysis of the velocity structure is not possible. Nevertheless, channel maps from 4 to 9 km s^{-1} reveal similar velocity patterns to those found in ^{13}CO. Peak temperatures in the CS maps reach 2 K in the NW clump, but they never exceed 1.1 K in the vicinity of HL Tau. At similar spectral and spatial resolution the peak ^{13}CO antenna temperature, 9.4 K, occurs at the stellar position. Integrated CS fluxes of 1.2 and 0.7 Jy km s^{-1} are found before and after continuum subtraction for $3 \leq V_{LSR} \leq 9$ km s^{-1}. No additional flux is obtained with wider velocity limits. For ^{13}CO we find 3.5 Jy km s^{-1} over $V_{LSR} = 3 \rightarrow 9$ km s^{-1}, which grows to 11 Jy km s^{-1} over $V_{LSR} = -6 \rightarrow 19$ km s^{-1}. At the NW source, the CS and ^{13}CO fluxes are each 1 Jy km s^{-1}, while at the S peak the CS and ^{13}CO fluxes are $\approx$0.5 and 1 Jy km s^{-1}. Thus, the CS/CO ratio is dramatically smaller in the central condensation.

3.3. *Single-Dish CS Observations*

The results from the single-dish observations are summarized in Table 1. No CS 5–4 and 7–6 emission was detected toward HL Tau at the CSO or IRAM; 2 σ upper limits are $T_A^* < 0.05$ and 0.07 K at the CSO, and 0.07 K for the 5–4 line at IRAM. The CS 2–1 and 3–2 lines were detected at IRAM toward HL Tau. However, at (+60″, 0) and (−120″, −120″)

TABLE 1

SUMMARY OF SINGLE-DISH OBSERVATIONS OF HL TAU

Line	Resolution (kHz)	$\int T_{MB}\,dV$ (K km s^{-1})	T_{MB} (K)	ΔV (km s^{-1})	V_{LSR} (km s^{-1})	Telescope	Beam
^{13}CO 2–1	50	7.39	4.26	1.63	6.40	CSO	30″
C^{18}O 2–1	50	0.89	0.67	1.25	6.54	CSO	30
CS 2–1	100	1.74[a]	1.30	1.26	6.58	IRAM	25
CS 2–1	100	0.89[a]	0.64	1.33	6.64	SEST	52
CS 3–2	500[b]	0.42	0.20	2.00	6.42	IRAM	17
CS 5–4	100	...	≤2.29	...	...	IRAM	12
	1000	...	≤0.14	...	...	IRAM	12
CS 5–4	50	...	≤0.28	...	...	CSO	28
	500	...	≤0.07	...	...	CSO	28
CS 7–6	500	...	≤0.10	...	...	CSO	20
				OFF (−2′,−2′)			
CS 2–1	100	1.37[a]	1.16	1.11	7.21	IRAM	25
CS 2–1	100	0.96[a]	0.61	1.47	7.00	SEST	52
CS 3–2	500[c]	...	≤0.11	...	...	IRAM	17

NOTE.—Upper limits are 2 σ.

[a] Calibration uncertain by 30%.

[b] Line not fully resolved.

1992ApJ...391L..99B

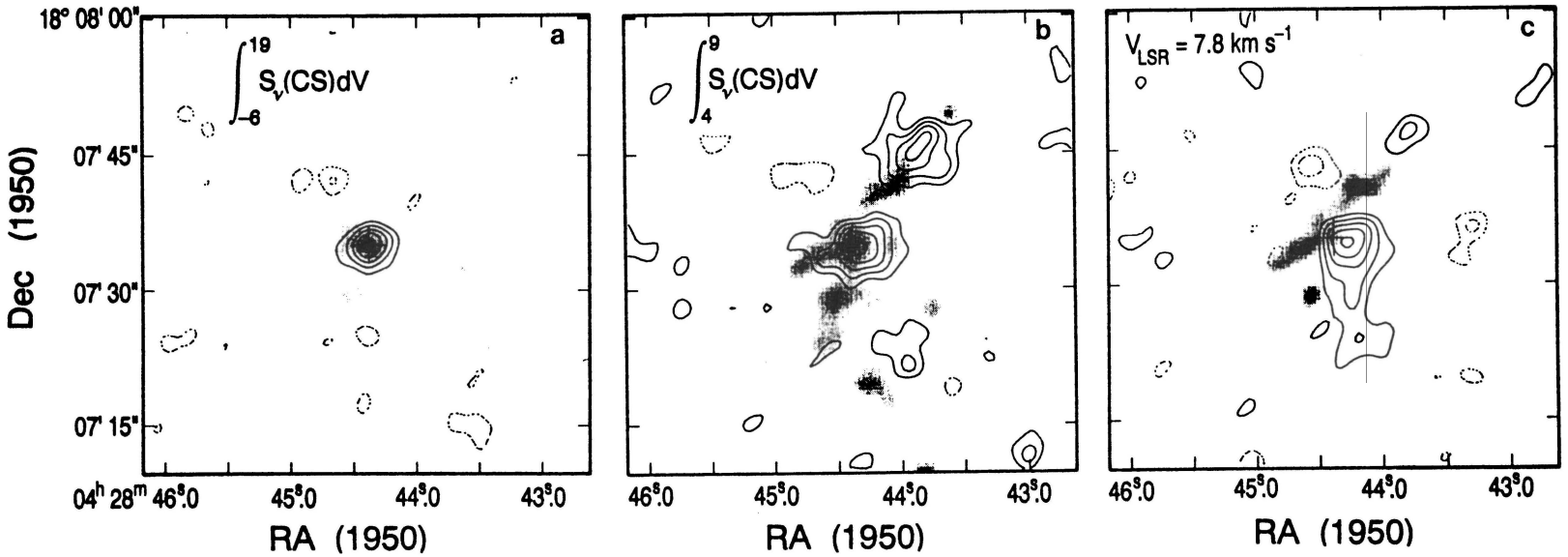

FIG. 1.—(*a*) CS $J = 2 \rightarrow 1$ (*contours*) and ^{13}CO $J = 1 \rightarrow 0$ (*gray scale*) emission from HL Tauri over the velocity range -6 to $+19$ km s^{-1}. Contours are at 30%, 45%, 60%, 75%, and 90% of the peak flux density, which is 2.1 Jy beam^{-1} km s^{-1}. Source size and peak flux density are nearly identical to that found in the 1150 km s^{-1} bandwidth continuum channel. The ^{13}CO gray scale runs from 0.6 to 7.0 Jy beam^{-1} km s^{-1} (Sargent & Beckwith 1991). A cross marks the position of HL Tauri in all panels. (*b*) As in (*a*) but integrated over the velocity range 4.1–9.0 km s^{-1}. Contours begin at the 1.5 σ level, 150 mJy beam^{-1} km s^{-1}, and are separated by 100 mJy beam^{-1} km s^{-1}. The peak CS flux density is 0.6 Jy beam^{-1} km s^{-1}. The ^{13}CO gray scale runs from 0.3 to 2.0 Jy beam^{-1} km s^{-1}. (*c*) CS emission in the 6.6–9.0 km s^{-1} range, clearly offset from the stellar position, along with ^{13}CO between 4.0 and 6.7 km s^{-1}. The peak CS flux density is 185 mJy beam^{-1}. Contours begin at 60 mJy beam^{-1} with a 30 mJy beam^{-1} interval (1 σ), and the ^{13}CO gray scale runs from 85 to 510 mJy beam^{-1}.

offset positions the 2–1 lines are very similar, although redshifted by about 0.5 km s^{-1}.

Spectra at the stellar position are centered at $V_{LSR} \approx 6.6$ km s^{-1}, but show no evidence for enhancement at $V_{LSR} \approx 8$ km s^{-1}, the velocity of the CS seen closest to HL Tau in the interferometer maps. Moreover, comparison of the IRAM CS 2–1 spectrum in a 25″ beam with a SEST spectrum in a 55″ beam shows at most a 40% difference in line strength. A similar lack of contrast between spectra taken at the stellar and offset positions is observed in other molecules such as HCO^+; only CO 3–2 observations reveal a significantly broader line at the stellar position (van Dishoeck et al. 1992b). The compact circumstellar disk contributes at most $T_{MB} \approx 0.2$ K to the CS 2–1 single-dish emission in a 25″ beam.

4. INTERPRETATION

4.1. *Dust Emissivity*

Estimates of disk masses are quite sensitive to the dust emissivity index β. Disk model fits to the infrared and submillimeter continuum emission may constrain β; it may be directly obtained from the long-wavelength thermal emission *only if* the bulk of the emission arises from optically thin material. Combining our 3.06 mm flux of 75 mJy with the fluxes obtained for HL Tau at 2.72 and 1.37 mm, 112 and 980 mJy (Sargent & Beckwith 1991, 1992), gives $\beta = 1.2 \pm 0.3$. This agrees well with the value derived from the disk models of Beckwith et al. (1990). Submillimeter continuum power-law fits give $\beta \sim 0.6$ (Weintraub, Sandell, & Duncan 1989; Adams, Emerson, & Fuller 1990; Beckwith & Sargent 1991). By assuming previously derived power-law distributions for the temperature and surface density of the circumstellar disk (Beckwith et al. 1990), we estimate a disk mass $M_D = 0.10\ M_\odot$ from the dust flux. Dust opacities reach unity at $r = 9$ AU in these models for $\lambda = 3.06$ mm. The derived mass is consistent with earlier observations and implies an average H_2 column density of 2×10^{24} cm^{-2} over a 3″ beam.

4.2. *CS Excitation*

The IRAM 2–1 and CSO 5–4, 7–6 single-dish data refer to fairly similar beams of 25″, 28″, and 20″. The resulting antenna temperature ratios are T(CS 2–1)/T(CS 5–4) $\gtrsim 15$ and T(CS 2–1)/T(CS 7–6) $\gtrsim 10$. These ratios are very different from those observed in dense regions such as Orion/KL (Blake et al. 1987), or even in other young stellar objects such as IRAS 16292 − 2422 (Menten et al. 1987) and T Tau (van Dishoeck et al. 1992b), where they are close to unity. Excitation calculations indicate that the ratios provide significant upper limits on the density of the CS-emitting region. For temperatures of 20 K or more, we find $n_{H_2} \lesssim 10^5$ cm^{-3}. Even at $T_{kinetic} = 10$ K, a density of at most 5×10^5 cm^{-3} is allowed. The best fit to the T(CS 2–1)/T(CS 3–2) ratio is for $n_{H_2} \approx 10^4$ cm^{-3}. These densities are much lower than predicted for the circumstellar disk, but are characteristic of the surrounding molecular cloud. For example, estimates of the densities in the nearby TMC-1 core range from a few times 10^4 to 10^5 cm^{-3} (Olano, Walmsley, & Wilson 1988). The inferred low-density is consistent with the fact that most of the single-dish emission seen toward HL Tau arises from extended material.

Our interferometer map indicates a central CS source size of less than 3″ in radius. Models of circumstellar disks such as the one surrounding HL Tau suggest n_{H_2} ranges from 10^{14} cm^{-3} at 1 AU to about 10^{10} cm^{-3} at 100 AU (Wood & Morfill 1989). Thus, at least up to a radius of 140 AU (1″ at HL Tau), the densities should be high enough to thermalize the CS excitation. The ^{13}CO emission is thought to be optically thick (Sargent & Beckwith 1991). If the CS emission in this central region also is optically thick and thermalized, it must be significantly more compact or arise from colder material. For $T_{kinetic} = 50$ K, comparable to the adopted dust temperature of $T_{dust} \approx 50$ K (Cohen 1983; Beckwith et al. 1986), the beam filling factor is 0.02, implying a diameter of order 0.″7 if the distribution is uniform. Lower temperatures would permit a somewhat larger size. Since the disk is probably highly flattened, and appears to be viewed nearly edge-on (Cohen 1983; Beckwith et al. 1989), a somewhat larger source radius is not implausible.

If the CS emission is optically thin, the observed line ratios constrain the source physical conditions. In particular, the nondetection of CS 5–4 is significant. Adopting a CS source radius of 3″ or less, the IRAM upper limit of $T_{MB} \leq 0.14$ K corresponds to $T_{MB} \leq 0.9$ K in a 4.″6 beam. Thus, we find that the 2–1/5–4 line ratio is $\gtrsim 1$ in the OVRO beam. Similarly, the CSO 7–6 upper limit indicates 2–1/7–6 $\gtrsim 1$ in the same beam. These ratios are consistent with thermal excitation only if the emitting gas is extremely cold, $T_{kinetic} \lesssim 15$ K. Such a low temperature is incompatible with the disk temperature structure inferred from continuum measurements. Of nearly 50 disk candidates studied by Beckwith et al. (1990), HL Tau is among the warmest, with a photospheric temperature of 300 K at 1 AU, decreasing to 15 K at $r = 400$ AU. Midplane temperatures are likely to be substantially higher given the predicted dust opacity. We can reconcile these two determinations only if we adopt a "hollow" structure, with gas-phase CS depleted from the part of the circumstellar material where the bulk of the CO emission originates.

Our temperature limits are also consistent with the CS emission arising from a region where $n_{H_2} \lesssim 10^6$ cm^{-3}, that is, near the molecular cloud/circumstellar disk interface. In simple models, this would place the CS-emitting region at distances of at least $r \gtrsim 450$ AU (3″ radius). The offset of the CS source in the continuum-subtracted images is consistent with this interpretation. Using similar arguments, we conclude that the other CS clumps seen in the interferometer map cannot have very high densities. Especially the NW clump, which appears to be extended over many arcseconds, must have $n_{H_2} \lesssim 10^5$ cm^{-3}.

4.3. *CS Abundance*

The CS abundance in the disk and molecular cloud can be derived from a comparison with the observed CO emission, provided that the lines are not too optically thick. For the surrounding dark cloud, the CSO ^{13}CO and $C^{18}O$ $J = 2$–1 spectra yield $N(H_2) \approx (2$–$3) \times 10^{21}$ cm^{-2} averaged over a 30″ beam. The inferred CS single-dish column density for $T_{kinetic} \approx 20$ K and $n_{H_2} \approx 10^4$ cm^{-3} is $N(CS) \approx (5 \pm 3) \times 10^{13}$ cm^{-2}, so that $x(CS) = N(CS)/N(H_2) \approx (1$–$2) \times 10^{-8}$, consistent with the CS abundance found in Taurus and other molecular clouds where $N(CS)/N(^{13}CO) \approx 0.01$.

Peak optical depths for the CS $2 \rightarrow 1$ emission from the molecular cloud reach 3.5 in our models, with similar optical depths for the ^{12}CO $1 \rightarrow 0$ transition. The ^{13}CO $1 \rightarrow 0$ line is optically thin. Characteristic line widths for the cold material are 1.3–1.7 km s^{-1} (Table 1), implying a visual extinction in the extended molecular cloud of $A_v \approx 2.5$–4 mag. For the HL

Tau/XZ Tau region, visual extinctions of order $A_v \approx 3.2$–3.5 mag have been derived (Cohen & Kuhi 1979; Beckwith et al. 1990). While it is difficult to determine the exact location of HL Tau with respect to the molecular cloud, it is likely that noticeable self-absorption of the ^{12}CO and CS will occur near line center. This may help explain the lack of CS emission near HL Tau in the central channels of the high-resolution filter bank. Absorption effects will *not* be important for ^{13}CO or for higher velocities in the ^{12}CO and CS maps where most of the system mass resides (Sargent & Beckwith 1991).

A rough estimate of the CS abundance in the *disk* can be obtained by comparing the integrated CS and ^{13}CO interferometer fluxes, and by assuming that the molecules are similarly distributed and that the lines are optically thin and thermalized. The ratio of integrated fluxes is then simply related to the ratio of the molecular partition functions (Q) and the inverse ratio of their Einstein A-values. CS has a dipole moment about a factor 16 larger than that for ^{13}CO, resulting in A(CS 2–1)/$A(^{13}\mathrm{CO}\ 1\text{–}0) = 267$. Q(CS)/Q(CO) is of order 2. The observed CS/^{13}CO flux ratio is approximately 0.1 without continuum subtraction and 0.06 with subtraction for the larger velocity ranges which sample the bulk of the circumstellar material. Thus, we find $N(\mathrm{CS})/N(^{13}\mathrm{CO}) \approx 4 \times 10^{-4}$, some 25 times lower than the value found for the extended molecular cloud surrounding HL Tau. In contrast, the CS/CO flux ratios in the NW and S clumps are consistent with those derived from the single-dish measurements, that is, with x(CS) $\approx$ a few times 10^{-9}.

If the ^{13}CO emission is optically thick and the CS emission is optically thin, the observed flux ratios provide a rough *upper* bound to the CS/CO abundance ratio of approximately 10^{-4}. For optically thick emission in both molecules, the line ratios demonstrate that the filling factor of the CS emission in 3″–4″ beams is significantly smaller than that for ^{13}CO. The compact nature of the continuum emission (and therefore the mass distribution) and the offset of the ^{13}CO and CS sources again argue for a true abundance difference. We believe that the gas-phase CS/CO ratio has been lowered substantially in the circumstellar disk. Either the CS has been depleted significantly onto grains, or it has been transformed chemically into other molecules.

Grain mantle depletion time scales range from well over 10^5 years to 10^4 yr at densities of 10^5 cm^{-3} for sticking coefficients α between 0.1 and 1.0, and they are therefore comparable to both chemical and dynamical time scales. At densities closer to 10^8 cm^{-3}, however, the grain depletion time scales have dropped to less than 30 yr if $\alpha = 1.0$. For dust temperatures near 50 K, virtually all molecules except species such as H_2, N_2, or CO will condense onto grains. In this context it is interesting to note that solid H_2O features have been observed toward HL Tau, while solid CO features have not (Whittet et al. 1989). The rather flat value of β compared to that of diffuse interstellar dust is consistent with substantial grain mantle growth via depletion. It may also reflect compositional evolution of grains in the star formation process (Beckwith & Sargent 1991).

The most likely CS loss processes in circumstellar disks involve the direct deposition of CS onto grain mantles or, if the gas phase atomic oxygen abundance is large, its conversion into CO by the reaction CS + O → CO + S, with subsequent depletion of S. In either case, grain mantles form the ultimate repository of sulfur in the outer regions of the circumstellar disk. Much closer to the central star ($r < 5$–10 AU), temperatures are high enough to drive the CS into H_2S. However, the high optical depth of the *dust* precludes the direct observation of the innermost disk for edge-on orientations. The observational study of high dipole moment molecules, which tend to possess the highest grain mantle binding energies, may therefore suffer both from dust opacity near the emission core and depletion over larger size scales, even at millimeter wavelengths.

Since the outer regions of T Tauri circumstellar disks have properties comparable to regions of the presolar nebula where comets presumably formed, a comparison of the derived CS abundance in the disk with that found in comets seems warranted. CS and CO have been detected in various comets through their ultraviolet lines (Feldman et al. 1986; Weaver et al. 1981; Jackson, Butterworth, & Ballard 1986). The CO abundance with respect to the principal constituent, H_2O, appears to vary from comet to comet with $CO/H_2O = 0.02$–0.2. Some temporal and spatial variations are also found for CS, but roughly $CS/H_2O \approx (2\text{–}10) \times 10^{-4}$. Assuming CO/^{13}CO ≈ 50, this would lead to CS/^{13}CO ≈ 0.05–2, significantly larger than the gas phase value found in interstellar clouds and in these observations of HL Tauri. However, the large CS/^{13}CO ratio may reflect the selective incorporation of CS versus CO in cometary ices or processing in the coma (Lunine 1989). The CS found in cometary atmospheres is thought to be a daughter product resulting from the photodissociation of CS_2, which along with H_2S forms the bulk of the molecular sulfur reservoir (the H_2CS abundance remains uncertain). If $H_2O/H_2 \approx 10^{-6}$ to 10^{-5} and complete retention is assumed, the cometary abundance ratio suggests $CS/H_2 \approx 10^{-9}$ to 10^{-8}. A possible scenario for the origin of cometary CS_2 is therefore interstellar CS depleted onto grain mantles and then converted into carbon disulfide, or possibly H_2CS if the mantles are hydrogen rich.

In the inner part of the solar nebula ($r \lesssim 5$–10 AU), most of the available sulfur is thought to be transformed into H_2S or pyrite (Barshay & Lewis 1976). The observed H_2S abundance in comets is $H_2S/H_2O \approx 0.002$ (Blockeleé-Morvan et al. 1990); or $H_2S/H_2 \approx (2\text{–}20) \times 10^{-9}$, which is again comparable to the average CS molecular cloud abundance. It appears unlikely, however, that CS can be carried into the inner nebula, transformed into H_2S, transported back to the outer nebula, and finally trapped in icy materials (Stevenson 1990). Searches for H_2S, H_2CS, and CS_2 on the surfaces of interstellar dust grains and laboratory experiments on the sulfur chemistry in synthetic grain mantles are needed to address the ultimate fate of CS once it enters the presolar nebula.

5. SUMMARY

We have presented high spatial and spectral resolution dust continuum and CS line-emission maps of the material immediately surrounding HL Tauri. The 3.06 mm thermal dust map gives an upper limit to the source size of roughly 200 AU. When combined with previous millimeter continuum measurements, a β value of 1.2 ± 0.3 is derived along with a disk mass of 0.1 $M_\odot$, in harmony with previous disk radiative transfer models of the IR and submillimeter flux from HL Tau. The low dust emissivity index as compared to particles in the diffuse ISM is best explained by grain growth or compositional evolution.

Our observations of the CS and CO emission lines from the molecular cloud surrounding HL Tauri are consistent with the

"canonical" temperatures, densities, and abundances derived in other Taurus cloud cores; namely $T \approx 10$–20 K, $n \approx 10^4$–10^5 cm^{-3}, and $x(\mathrm{CS}) = (1\text{–}2) \times 10^{-8}$. In contrast, the CS emission in aperture synthesis maps at 650 AU spatial resolution is most consistent with CS/CO ratios at least 25–50 times lower in the gas immediately surrounding HL Tauri if the CS emission is optically thin. For optically thick CS emission, the smaller filling factor relative to ^{13}CO and the source structure also argue for a depleted CS abundance. Lowered CS abundances are most likely the result of depletion of molecules onto dust grain mantles, but conversion of gas-phase CS into other sulfur-containing species may also occur, especially in the inner part. The continuum and spectral line results obtained are strong indicators of conditions thought to be similar to those in the presolar nebula some 4.5 A.E. ago.

The authors are grateful to the CSO, IRAM, and OVRO staff, and in particular P. G. Green, for providing assistance during the observations. They are also indebted to R. Gredel for obtaining the SEST CS 2–1 spectra. The CSO and OVRO are operated under funding from the NSF, contracts 90-15755 and 90-16404. This work was also supported through NASA grants NAGW-1945 and 2297. G. A. B. gratefully acknowledges financial support provided by the David and Lucille Packard and Alfred P. Sloan Foundations. E. v. D. is indebted to the Netherlands Organization for Scientific Research.

REFERENCES

Adams, F. C., Emerson, J. P., & Fuller, G. A. 1990, AJ, 357, 606
Barshay, S. S., & Lewis, J. S. 1976, ARA&A, 14, 81
Beckwith, S. V. W., & Sargent, A. I. 1991, ApJ, 381, 250
Beckwith, S. V. W., Sargent, A. I., Chini, R. S., & Güsten, R. 1990, AJ, 99, 924
Beckwith, S. V. W., Sargent, A. I., Koresko, C. D., & Weintraub, D. A. 1989, ApJ, 343, 393
Beckwith, S. V. W., Sargent, A. I., Scoville, N. Z., Masson, C. R., Zuckerman, B., & Phillips, T. G. 1986, ApJ, 309, 755
Blake, G. A., Sutton, E. C., Masson, C. R., & Phillips, T. G. 1987, ApJ, 315, 621
Bockelée-Morvan, D., et al. 1990, in Formation of Stars and Planets, and the Evolution of the Solar System, ed. B. Battrick (SP-215) (Noordwijk: ESA), 143
Cohen, M. 1983, ApJ, 270, L69
Cohen, M., & Kuhi, L. V. 1979, ApJS, 48, 743
Elias, J. H. 1978, ApJ, 224, 857
Feldman, P. D., et al. 1986, in Proc. 20th ESLAB Symp. The Exploration of Halley's Comet (ESA SP-250) (Noordwijk: ESA), 325
Jackson, W. M., Butterworth, P. S., & Ballard, D. 1986, ApJ, 304, 515
Lunine, J. I. 1989, Icarus, 81, 1
Menten, K. M., Serabyn, E., Güsten, R., & Wilson, T. L. 1987, 117, L57
Ohashi, N. Kawabe, R., Hayashi, M., & Ishiguro, H. 1991, AJ, 102, 2054
Olano, C. A., Walmsley, C. M., & Wilson, T. L. 1988, A&A, 196, 194
Sargent, A. I., & Beckwith, S. 1987, ApJ, 323, 294
———. 1991, ApJ, 382, L31
———. 1992, in preparation
Shu, F. H., Adams, F. C., & Lizano, S. 1987, ARA&A, 25, 23
Stevenson, D. J. 1990, ApJ, 348, 730
Strom, K., Strom, S. E., Edwards, S., Cabrit, S., & Strutskie, M. 1989, AJ, 97, 1451
Strom, S. E., Edwards, S., & Strutskie, M. 1992, in Protostars and Planets III, ed. E. H. Levy, J. I. Lunine, & M. S. Mildred (Tucson: Univ. Arizona), in press
van Dishoeck, E. F., Blake, G. A., Draine, B. T., & Lunine, J. I. 1992a, in Protostars and Planets III, ed. E. H. Levy, J. I. Lunine, & M. S. Mildred (Tucson: Univ. Arizona), in press
van Dishoeck, E. F., et al. 1992b, in preparation
Weaver, H. A., et al. 1981, Icarus 47, 449
Weintraub, D. A., Masson, C. R., & Zuckerman, B. 1989, ApJ, 344, 915
Weintraub, D. A., Sandell, G., & Duncan, W. D. 1989, ApJ, 340, L69
Whittet, D. C. B., et al. 1989, MNRAS, 241, 707
Wood, J. A., & Morfill, G. 1989, in Meteorites and the Early Solar System, ed. J. F. Kerridge & M. S. Matthews (Tucson: Univ. Arizona), 329